

Molecular Rotation and Polarization under Thermal Gradients

Alpha A Lee^{1,2,*}

¹*John A. Paulson School of Engineering and Applied Sciences,
Harvard University, Cambridge, MA 02138, USA*

²*Mathematical Institute, Andrew Wiles Building, University of Oxford,
Woodstock Road, Oxford OX2 6GG, United Kingdom*

Recent molecular dynamics simulations show that a thermal gradient induces an electric field in water that is comparable to that seen in ionic thin films and biomembranes. This counterintuitive phenomena of thermo-orientation is also observed more generally in simulations of polar and non-polar size-asymmetric dumbbell fluids. However, a microscopic theory for this novel non-equilibrium phenomenon is yet unknown. We develop a microscopic theory of thermo-orientation using a mean-field, local equilibrium approach. Our theory reveals analytically how thermo-orientation depends on the molecular volume, size anisotropy, and dipole moment. Predictions of the theory agree quantitatively with molecular dynamics simulations. Crucially, our framework shows how thermo-orientation can be controlled and maximised by tuning microscopic molecular properties.

Non-equilibrium effects play an important role in processes relevant to biology, chemistry, physics and materials science. In particular, temperature gradients often trigger a plethora of coupling effects. It is well known that thermal gradients trigger mass transport, commonly known as the Soret effect [1]. Colloids in a suspension tend to move towards colder regions, and the thermophoretic response of a molecule depends on molecular properties such as charge and size [2]. This effect allows mixtures of nanoscopic particles and biomolecules to be separated efficiently [3–6].

Recent molecular dynamics simulations have shown that, analogous to the Soret effect, thermal gradients can trigger a preferential orientation if the molecule is anisotropic [7]. Diatomic molecules with a larger “head” and a smaller “tail” rotate in response to a thermal gradient, with the “fatter” end of the molecule pointing towards the hot region (see Figure 1). If the molecules are polar, this preferential orientation can induce a significant electric field. For liquid water, the thermoelectric field can be $\sim 10^6$ V/m for temperature gradients of the order of $\sim 10^8$ K/m [8]. These electric fields are characteristic of ionic thin films and biomembranes, and the large thermal gradients can be generated by nanoparticle systems that experience heating from absorption of electromagnetic radiation. Therefore, this effect of hot water polarisation may be relevant in proposals of destroying cancer cells with nanoparticles and radiation sources [8, 9].

However, a microscopic theory that relates molecular properties, such as the degree of anisotropy and dipole moment, to the extent of reorientation and magnitude to electric field generated is yet unknown. Prior studies of thermal reorientation rely on positing linear flux-force relations and introducing phenomenological Onsager’s coefficients. The insight that phenomenological relations have revealed is the dependence of the response field to local temperature and thermal gradient: in a non-polar liquid, $\langle \cos \theta_x \rangle$ is directly proportional to the thermal

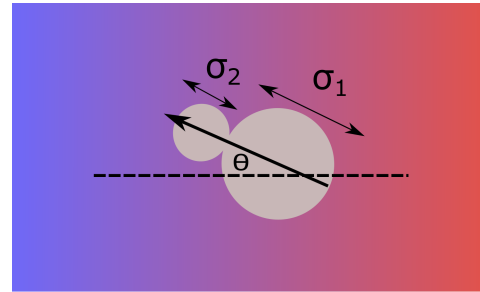


FIG. 1: Schematic sketch of the system under consideration: a model anisotropic molecule consisting of two touching spheres of diameters σ_1 and σ_2 in a thermal gradient.

gradient and inversely proportional to the local temperature, where θ is the angle between the x -axis and the orientation vector \mathbf{n} of a molecule (defined to be a unit vector in the direction of the molecular axis pointing from the larger end to the smaller end), and the thermal gradient applied in the x -direction [7]. For polar liquids, the induced electric field \mathbf{E} scales inversely with temperature and linearly with thermal gradient [8].

In this Letter, we will first derive the relationship between microscopic molecular properties and thermomolecular reorientation of a model non-polar molecule using a local equilibrium approach. We will then extend the theory to consider thermal polarisation of polar molecules. Our results will be verified through comparison with non-equilibrium molecular dynamics simulations. Underlying our approach, we argue that molecular rotation and polarisation under thermal gradients is an extension of the Soret effect: the torque exerted on an anisotropic molecule is due to a Soret force pushing the larger end of the molecule to warmer region, and the smaller end to colder region.

Consider first a simpler problem of thermophoresis of a hard sphere suspension. We will use the local equilibrium approach, and assume that the equilibrium free

energy and chemical potential continue to be valid outside equilibrium, but with the temperature replaced by the local temperature [3, 10, 11]. A simple model is that the free energy is proportional to the exposed surface area (a solvation model),

$$G_{\text{solv}} = -k_B T s \sigma^2, \quad (1)$$

where σ is the hard sphere diameter, and s is a positive constant if we assume that the solute is solvophilic (hence demixing is thermodynamically unfavourable) and negative vice versa. A thermal gradient therefore creates a spatially varying free energy, and the molecules moves along the chemical potential gradient. Substituting Equation (1) into the well-known relation in local equilibrium theory between Soret coefficient and free energy, $S_T = (dG/dT)/(k_B T)$ [10, 11], yields $S_T = -s\sigma^2$. This linear dependence of the Soret coefficient on molecular area agrees with experimental observations [12], showing that (1) is a reasonable model for the free energy despite its simplicity. The local equilibrium picture in thermophoresis holds as long as molecules are in mechanical equilibrium (*i.e.* no acceleration), which is almost always the case due to large viscous dissipation [13, 14].

A single hard sphere evidently cannot display thermomolecular orientation. The crucial ingredient missing is shape anisotropy, which can be realised by joining two touching hard spheres of different diameters (see Figure 1). Local equilibrium approach can now be applied to thermo-molecular reorientation. Assuming that the form for the free energy does not change for a dumbbell, the total free energy of the dumbbell molecule is simply the sum of G_{solv} for the large and small spheres, but crucially with different temperatures because the spheres are in the thermal gradient

$$G_{\text{tot}} = -k_B s (T_1 \sigma_1^2 + T_2 \sigma_2^2), \quad (2)$$

where $T_{1,2}$ is the local temperature at dumbbell 1/2. Physically, the lengthscale of temperature variation is much larger than the length of the molecule. Therefore, $T_{1,2}$ is related to the local temperature T and gradient $\nabla_x T$ at the midpoint of the molecule via

$$\begin{aligned} T_1 &\approx T + \frac{l}{2} \cos \theta \nabla_x T, \\ T_2 &\approx T - \frac{l}{2} \cos \theta \nabla_x T, \end{aligned} \quad (3)$$

where $l = \sigma_1 + \sigma_2$ is the length of the molecule. (For linear temperature gradients, Equation (3) holds identically.) The average orientation $\langle \cos \theta_x \rangle$ can be computed by a Boltzmann average

$$\begin{aligned} \langle \cos \theta_x \rangle &= \frac{\int_0^\pi \cos \theta \sin \theta e^{-\frac{G_{\text{tot}}}{k_B T}} d\theta}{\int_0^\pi \sin \theta e^{-\frac{G_{\text{tot}}}{k_B T}} d\theta}, \\ &= \frac{\int_0^\pi \cos \theta \sin \theta \exp \left[-\frac{sl}{2T} \cos \theta (\sigma_2^2 - \sigma_1^2) \nabla_x T \right] d\theta}{\int_0^\pi \sin \theta \exp \left[-\frac{sl}{2T} \cos \theta (\sigma_2^2 - \sigma_1^2) \nabla_x T \right] d\theta}. \end{aligned} \quad (4)$$

In the linear response regime, $\nabla_x T \ll 1$, and the integrals in Equation (4) can be evaluated to give

$$\langle \cos \theta_x \rangle \approx \frac{1}{6} sl \frac{\nabla_x T}{T} \sigma_2^2 \left[\left(\frac{\sigma_1}{\sigma_2} \right)^2 - 1 \right]. \quad (5)$$

Assuming a fixed molecule length l , Equation (5) shows that $\langle \cos \theta_x \rangle$ is related to the size asymmetry ratio $\chi = \sigma_2/\sigma_1$ via

$$\langle \cos \theta_x \rangle = \frac{sl^3}{6} \frac{\chi - 1}{\chi + 1} \frac{\nabla_x T}{T}. \quad (6)$$

Equation (6) is a central result of this Letter. It shows that the thermomolecular reorientation depends on both the size asymmetry of the molecule and molecular volume. The only unknown in Equation (6) is the relationship between s , the solvation energy per unit exposed surface area, and χ . Simulations [15] show that phase diagram of size-asymmetric hard dumbbells collapse onto a single one when the temperature and density are scaled with the corresponding critical values. Indeed, the critical temperature is a measure of the (entropic) interactions that render the fluid state stable, and as such we assume that $s \propto T_{\text{crit}}$. Figure 2 shows that the polarisation obtained from simulation quantitatively agrees with this scaling: $\langle \cos \theta_x \rangle \propto (\chi - 1)/(\chi + 1)$ when the temperature is expressed in terms of the critical temperature. Increasing the temperature by a factor of 1.2 increases the prefactor by a factor of 1.3, close to the expected scaling. Furthermore, Equation (6) predicts that the reorientation effect depends rather weakly on χ for large χ , yet scales linearly with l^3 , the molecular volume. Those scalings suggest that in order to engineering the strongest reorientation effect, it is more important to use large molecules than ones with large size anisotropy.

For dipolar, size-assymmetric molecules, molecular rotation under thermal gradients generates a concomitant electric field. This electric field can be estimated using a self-consistent mean-field approximation. Analogous to the approach above, we first note that the free energy of a size-asymmetric dipole of dipole moment μ in a thermal gradient with an electric field E (which will be computed later by imposing self-consistency) is given by

$$G_{\text{tot}} = -k_B s (T_1 \sigma_1^2 + T_2 \sigma_2^2) + \mu E \cos \theta. \quad (7)$$

Following the approach for uncharged dumbbells, the average orientation is given by (*c.f.* Equation (4))

$$\langle \cos \theta_x \rangle = \frac{1}{6} sl \frac{\nabla_x T}{T} \frac{\chi - 1}{\chi + 1} - \frac{1}{3k_B T} \mu E. \quad (8)$$

The electric field E needs to be determined self-consistently. Noting the classical relation between polarisation and electric field $E = -4\pi P$, we obtain

$$E = 4\pi \rho \mu \langle \cos \theta_x \rangle, \quad (9)$$

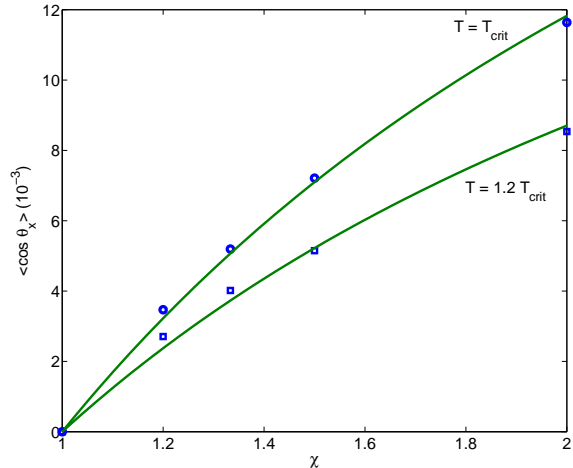


FIG. 2: Comparison of our theory with non-equilibrium molecular dynamics simulations of Lennard-Jones dumbbells [15]. In those simulations the gradient $\nabla_x T = 1K/\text{\AA}$ is kept constant, and the temperature is scaled to the corresponding critical value for given χ . The function $A(\chi - 1)/(\chi + 1)$ (green solid line, c.f., Equation (6)) can be fitted (using A) to simulation data (open circles and squares) with $A = 0.035$ ($T = T_{\text{crit}}$) and $A = 0.026$ ($T = 1.2 T_{\text{crit}}$) (note that the average orientation for $\chi = 1$ is used as the zero baseline to calibrate errors in simulations).

where ρ is the dipole density. Substituting Equation (9) into Equation (8), we obtain

$$E = \frac{\frac{2\pi\rho}{3}sl\mu}{1 + \frac{4\pi\rho}{3k_B T}\mu^2} \frac{\chi - 1}{\chi + 1} \frac{\nabla_x T}{T}. \quad (10)$$

Equation (10) predicts that the induced electric field is a non-monotonic function of dipole moment. This is a result of two competing effects. On one hand, electric field can be induced only for systems with a non vanishing dipole moment, and by symmetry we have $E \propto \mu$. On the other hand, when the dipole moment increases, the dipoles become strongly correlated even at no applied thermal field. Though a net electric field is absent, each dipole is locally strongly solvated by other dipoles. Indeed, there is a net attractive interaction between dipoles whose orientations are thermally averaged, and this is the origin of the Keesom interaction [16, 17]. Therefore, a large thermal gradient is needed to rotate the dipole amid its solvation atmosphere and induce an electric field. Figure 3 shows that average orientation predicted by the theory (related to Equation (10) via Equation (9)) is in quantitative agreement with simulation data [18]. Equation (10) affords the crucial insight that the induced electric field is maximised when the dipole moment equals $\mu_{\text{max}} = \sqrt{4\pi\rho/(3k_B T)}$. In a hard-sphere molecular fluid, changing the dipole moment changes the equation of state and thus the dependence of ρ on T . Nonetheless, the optimality condition

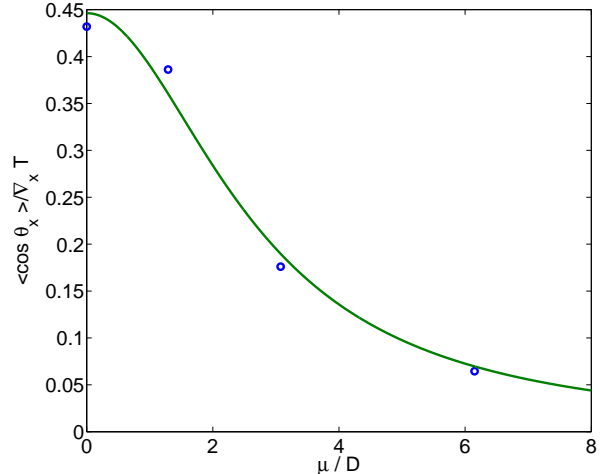


FIG. 3: The maxima in the average orientation of dipolar Lennard-Jones dumbbells in response to an applied thermal gradient obtained using non-equilibrium molecular dynamics simulations [18] can be fitted quantitatively to Equation (10). In those simulations the gradient $\nabla_x T = 1K/\text{\AA}$ is kept constant. The function $A/(1 + B\mu^2)$ can be fitted (using A and B) to simulation data (open circles) with $A = 0.45$ and $B = 0.14$. Note that $\langle \cos \theta_x \rangle$ is related to E via Equation (9)

between dipole moment, density and temperature could be attained via introducing other non-electrostatic intermolecular interactions such as van der Waals forces and specific chemical interactions.

In summary, we have derived a microscopic theory of molecular rotation and polarisation under thermal gradients by using a local equilibrium approach with a simple solvation free energy. In particular, we show that for non-polar molecules, the reorientation effects not only depends on degree of size asymmetry, but also increases linearly with the molecular volume. For polar molecules, the induced electric field is a non-monotonic function of the dipole moment, with $\mu_{\text{max}} = \sqrt{4\pi\rho/(3k_B T)}$ being the global optimal. The predictions of the theory agrees quantitatively with simulation data. Thus our results provide novel ways to control and enhance the extent of polarisation and reorientation by relating the magnitude of the effect to microscopic molecular properties.

This work was supported by an EPSRC Research Studentship and a Fulbright Fellowship to AAL.

* Electronic address: alphalee@g.harvard.edu

- [1] S. R. de Groot and P. Mazur, *Non-equilibrium thermodynamics* (Dover Publications, 2011).
- [2] R. Piazza, *Soft Matter* **4**, 1740 (2008).
- [3] S. Duhr and D. Braun, *Proceedings of the National Academy of Sciences* **103**, 19678 (2006).
- [4] C. J. Wienken, P. Baaske, U. Rothbauer, D. Braun, and

- S. Duhr, Nature communications **1**, 100 (2010).
- [5] Y. T. Maeda, T. Tlusty, and A. Libchaber, Proceedings of the National Academy of Sciences **109**, 17972 (2012).
- [6] A. Lervik and F. Bresme, Physical Chemistry Chemical Physics **16**, 13279 (2014).
- [7] F. Römer, F. Bresme, J. Muscatello, D. Bedeaux, and J. M. Rubí, Physical Review Letters **108**, 105901 (2012).
- [8] F. Bresme, A. Lervik, D. Bedeaux, and S. Kjelstrup, Physical Review Letters **101**, 020602 (2008).
- [9] P. K. Jain, I. H. El-Sayed, and M. A. El-Sayed, Nano Today **2**, 18 (2007).
- [10] E. Eastman, Journal of the American Chemical Society **48**, 1482 (1926).
- [11] E. Eastman, Journal of the American Chemical Society **50**, 283 (1928).
- [12] S. Duhr and D. Braun, Physical Review Letters **96**, 168301 (2006).
- [13] R. D. Astumian, American journal of physics **74**, 683 (2006).
- [14] R. D. Astumian, Proceedings of the National Academy of Sciences **104**, 3 (2007).
- [15] F. Römer and F. Bresme, Molecular Simulation **38**, 1198 (2012).
- [16] W. Keesom, Proc. R. Acad. Amsterdam **18**, 636 (1915).
- [17] J. N. Israelachvili, *Intermolecular and surface forces* (Academic press, 2011), 3rd ed.
- [18] C. D. Daub, P.-O. Åstrand, and F. Bresme, Physical Chemistry Chemical Physics **16**, 22097 (2014).